

## Investigating the effect of self-trapped holes in the current gain mechanism of $\beta$ -Ga<sub>2</sub>O<sub>3</sub> Schottky diode photodetectors

Fatih AKYOL\* 

Department of Metallurgical and Materials Engineering, Faculty of Chemical and Metallurgical Engineering, Yıldız Technical University, İstanbul, Turkey

Received: 09.02.2021

Accepted/Published Online: 05.04.2021

Final Version: 28.06.2021

**Abstract:** Monoclinic gallium oxide ( $\beta$ -Ga<sub>2</sub>O<sub>3</sub>) has found great research interest in solar blind photodetector (SBP) applications due to its' bandgap  $\sim 4.85$  eV and availability of high quality native crystal growth. Applications including missile guidance, flame detection, underwater/intersatellite communication and water purification systems require SBPs.  $\beta$ -Ga<sub>2</sub>O<sub>3</sub> SBPs with high responsivity values have been published indicating internal gain in these devices. The gain has been attributed to accumulation of self-trapped hole (STH) below Schottky metal which the lowers Schottky barrier in these devices based on some approximations rather than a proper device simulation. In this paper, technology computer-aided design (TCAD) simulation of  $\beta$ -Ga<sub>2</sub>O<sub>3</sub> SBPs are performed to numerically investigate the effect of low hole mobility STHs on Schottky barrier lowering (SBL). The simulations revealed that based on the theoretical hole mobility of  $1 \times 10^{-6} \text{ cm}^2\text{V}^{-1}\text{s}^{-1}$ , photoconductive gain in  $\beta$ -Ga<sub>2</sub>O<sub>3</sub> based photodetectors cannot be attributed to STH related hole accumulation near Schottky contact. It is found that hole mobility in the range of  $1 \times 10^{-10} \text{ cm}^2\text{V}^{-1}\text{s}^{-1} - 1 \times 10^{-12} \text{ cm}^2\text{V}^{-1}\text{s}^{-1}$  is required to induce  $\sim 0.3$  eV of SBL potential. Unless such low hole mobility is reported either experimentally or theoretically, it is not reasonable to attribute gain to STH formation in these devices.

**Key words:** Gallium oxide,  $\beta$ -Ga<sub>2</sub>O<sub>3</sub> self-trapped holes, photodetector, Schottky barrier lowering, photoconductive gain, simulation

### 1. Introduction

Solar blind photodetectors (SBPs) have been focus of research owing to potential applications in underwater and intersatellite communications, missile guidance and water purification systems. Having band gap energy  $\sim 4.85$  eV, and high quality melt grown substrate availability,  $\beta$ -Ga<sub>2</sub>O<sub>3</sub> is one of the most promising wide band gap material which is suitable for applications in SBPs [1-4]. Also, various thin film growth techniques have been successfully performed to modify dopants as well as to get heteroepitaxial layers on various substrates [5-8]. From these materials various SBP devices have been reported, mostly in the form of Schottky and metal-semiconductor-metal (MSM) architecture [9-14]. In general, the devices show large photoconductive gain that is the number of electrical charges flowing from the device is larger than number of the incident photons. In many reports the gain is obtained even at low bias range (1-5 V) [10-12] and in some devices; gain is observed with an onset at high bias ( $> 10$  V) condition [13-15]. The latter case indicates clearly that impact ionization is the gain mechanism in those devices. On the other hand, explaining the former case has been controversial.

\*Correspondence: [akyolf@yildiz.edu.tr](mailto:akyolf@yildiz.edu.tr)

Without direct experimental proof, it was speculated to be due to hole traps near Schottky contact. Widely accepted explanation for the gain has been related with the presence of self-trapped holes (STHs) [14].

Theoretical studies indicated that holes have very high hole effective mass and those are trapped by localized lattice distortions in  $\beta$ -Ga<sub>2</sub>O<sub>3</sub> and such phenomenon results in very low hole mobility estimated to be  $1 \times 10^{-6} \text{ cm}^2\text{V}^{-1}\text{s}^{-1}$  based on activated process in a STH migration process [15,16]. Experimental works also supported the STH formation through photocurrent spectroscopy [16], electron paramagnetic resonance [17] and photo-luminescence [18] measurements on n-type  $\beta$ -Ga<sub>2</sub>O<sub>3</sub>. On the other hand, recently p-type conductivity in hydrogen doped  $\beta$ -Ga<sub>2</sub>O<sub>3</sub> and heavily N-doped  $\beta$ -Ga<sub>2</sub>O<sub>3</sub> (hole mobility of  $41.4 \text{ cm}^2\text{V}^{-1}\text{s}^{-1}$ ) have been demonstrated [19,20]. Also, simulations on  $\beta$ -Ga<sub>2</sub>O<sub>3</sub> based photodetectors revealed average hole mobility of  $20 \text{ cm}^2\text{V}^{-1}\text{s}^{-1}$  [21]. These indicate that applied electric field, material growth conditions and doping elements can greatly effect hole transport mechanism in  $\beta$ -Ga<sub>2</sub>O<sub>3</sub>.

One of the most highly cited study has been performed by Armstrong et al. on the role of STHs in photoconductive gain of  $\beta$ -Ga<sub>2</sub>O<sub>3</sub> detectors [14]. The work was based on the generation of excess positive charge near Schottky contact assuming an optical absorption coefficient of  $10^7 \text{ cm}^{-1}$  for  $h\nu > 5 \text{ eV}$ . With simple calculation authors reported the STH formation with a concentration of  $1 \times 10^{19} \text{ cm}^{-3}$  below  $\beta$ -Ga<sub>2</sub>O<sub>3</sub> surface upon above bandgap illumination. However, the reference used for such high optical absorption coefficient in fact reported the value  $\sim 10^7 \text{ m}^{-1}$  (probably a unit conversion mistake) which is 100 times less than the value used in the abovementioned study [22]. Considering this difference, the reported STH concentration will decrease by 100 times which would result in no considerable change in Schottky barrier height lowering (SBL) thus, could not satisfactorily explain gain in  $\beta$ -Ga<sub>2</sub>O<sub>3</sub> based photodetectors. A proper device simulation is needed to investigate the effect of hole mobility (STH) on the photoconductive gain of  $\beta$ -Ga<sub>2</sub>O<sub>3</sub> detectors.

In this report the effect of STH mobility on SBL is simulated by TCAD software based on widely accepted  $\beta$ -Ga<sub>2</sub>O<sub>3</sub> material parameters to solve drift diffusion and carrier continuity equations upon ultraviolet excitation, hole mobility variation and reverse biasing. Recombination mechanisms firstly investigated then, hole concentration level was analysed. After investigating the electric field profile SBL potential was calculated. The results were discussed to identify the relation between the photoconductive gain and STH related low hole mobility in  $\beta$ -Ga<sub>2</sub>O<sub>3</sub> detectors.

## 2. Methods

Having low hole mobility, holes are expected to accumulate in depletion region of a Schottky diode. Combined with the ionized donor charge, negative image charge in Schottky metal builds up to satisfy charge neutrality. This negative charge effectively lowers the barrier height between metal and semiconductor ( $\phi_b$ ) by a value of  $\Delta\phi_b$  (Figure 1a) which is defined by the following equation [23,24]:

$$\Delta\phi_b = \sqrt{\frac{q E_m}{4 \pi \epsilon_s}}, \quad (1)$$

where  $E_m$  is the electric field strength in a semiconductor at the metal interface and  $\epsilon_s$  is dielectric constant of the semiconductor. It can be seen from Eq. (1) that electric field should be calculated to find barrier lowering potential. Note that optically generated minority carrier hole density need to be considered in electric field calculation especially in semiconductors under photo excitation with low hole mobility (in the case of STH based transport). To do this task, a proper device simulation should be used.

The simulations of STH mobility on SBL of  $\beta\text{-Ga}_2\text{O}_3$  vertical SBPs are obtained by solving drift-diffusion, carrier continuity and Shockley-Read-Hall (SRH) recombination equations using Silvaco Atlas semiconductor device software. Following material parameters were used to model of  $\beta\text{-Ga}_2\text{O}_3$  in this work; energy band gap of 4.8 eV [25], electron affinity of 4 eV [26], relative dielectric constant of 10 [27], optical absorption coefficient of  $5 \times 10^5 \text{ cm}^{-1}$  [22], electron mobility of  $153 \text{ cm}^2\text{V}^{-1}\text{s}^{-1}$  [28], electron effective mass of  $0.28 m_0$  [29] and minority carrier hole and electron lifetime of 0.176 ns [30]. Above band gap excitation energy of 5 eV was used with a power density of  $1 \text{ mWcm}^{-2}$ . Schottky barrier height of 1.05 eV was set and 100% metal optical transparency was assumed for simplicity [31]. The simulated structure is depicted in Figure 1b. The structure had  $2 \mu\text{m}$  thick  $3 \times 10^{17} \text{ cm}^{-3}$  n-type doped  $\beta\text{-Ga}_2\text{O}_3$  layer with full Schottky metal coverage on front side and ohmic contact on the back side. It is assumed that donors fully ionize in the n-type layer.

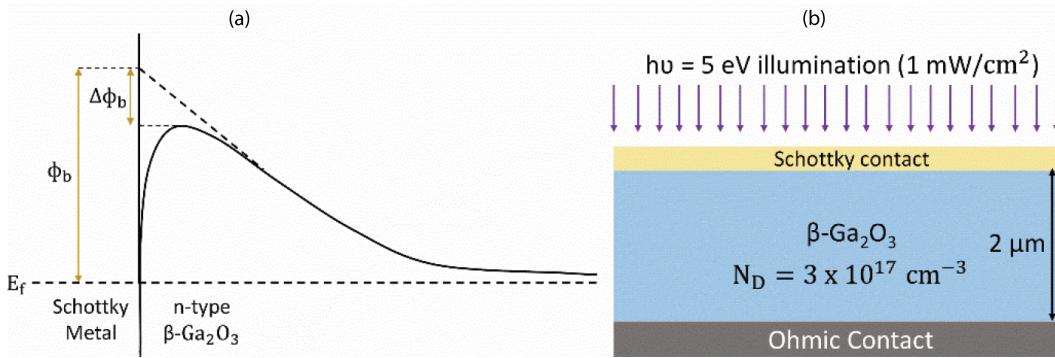


**Figure 1.** (a) Schematic representing Schottky barrier lowering in a Schottky diode. (b) The design of the simulated Schottky diode.

### 3. Results and discussion

In the simulation, the effect of STH formation is represented by low hole mobility which reflects itself with two main process; (1) high Shockley-Read-Hall (SRH) recombination rate at positions away from Schottky contact under weak electric field strength and (2) high concentration of holes at positions close to Schottky contact where hole drift current flows. Having high electric field near Schottky contact depicts itself with aforementioned Schottky barrier lowering. To investigate this whole process, we can start from investigating the simulation of SRH recombination rate using the following equation [32];

$$R_{\text{SRH}} = \frac{p n - n_{\text{ie}}^2}{\tau_n [n + n_{\text{ie}} \exp(E_T/kT)] + \tau_p [p + n_{\text{ie}} \exp(-E_T/kT)]}, \quad (2)$$

where  $p$ ,  $n$  and  $n_{\text{ie}}$  are hole, electron and intrinsic carrier concentrations, and  $k$ ,  $T$  are Boltzmann constant and lattice temperature, respectively. Electron and hole minority carrier lifetimes are denoted by  $\tau_n$  and  $\tau_p$ , respectively. Parameter  $E_T$  represents the energy difference between trap and intrinsic energy level which is assumed to be 0 eV in the simulation. Then, the term ' $n + n_{\text{ie}} \exp(E_T/kT)$ ' reduces to ' $n + n_{\text{ie}}$ ' and since  $n \gg n_{\text{ie}}$  for n-type semiconductors, the term further reduces to ' $n$ '. Similar steps applies to holes upon above bandgap optical excitation. Since,  $p \times n \gg n_{\text{ie}}^2$  under these conditions. Finally, Eq. (2) approximately equals to the flowing;

$$R_{\text{SRH}} \cong \frac{p n}{\tau_n n + \tau_p p}. \quad (3)$$

The variation of simulated SRH rate, electron and hole concentrations and applied optical generation rate with the distance from the Schottky contact is shown in Figure 2a for the SBP with hole mobility of  $1 \times 10^{-6} \text{ cm}^2\text{V}^{-1}\text{s}^{-1}$  under zero bias condition. It can be seen that SRH rate peaked up to the optical recombination rate at the position where electron and hole concentrations are equal to each other. This relation is expected from Eq. (3) where ' $R_{\text{SRH}}$ ' has its maximum value at ' $p = n$ ' condition. The situation of SRH rate being equal to the optical generation rate indicates that none of the optically generated holes contributes to photocurrent and all of these get recombined with majority carrier electrons at the given position. As the vertical distance from the Schottky contact decreases below  $\sim 25 \text{ nm}$ , the hole concentration rapidly increases. Holes at this region are able to drift to the Schottky contact as expected from a photodiode.

The effect of hole mobility on SRH rate characteristic is critical especially at very low hole mobility levels. Variation of SRH recombination rate and electron concentration across vertical distance from Schottky contact is depicted in Figure 2b under varying hole mobility values from  $1 \times 10^{-6} \text{ cm}^2\text{V}^{-1}\text{s}^{-1}$  down to  $1 \times 10^{-12} \text{ cm}^2\text{V}^{-1}\text{s}^{-1}$ . As expected, further lower hole mobility resulted in expansion of SRH recombination over the device, especially in regions with relatively lower Electric field. This is also verified from electron concentration profile (Figure 2b). At hole mobility values lower than  $1 \times 10^{-8} \text{ cm}^2\text{V}^{-1}\text{s}^{-1}$ , electron concentration increases which obviously boosts SRH rate (Eq. 3).

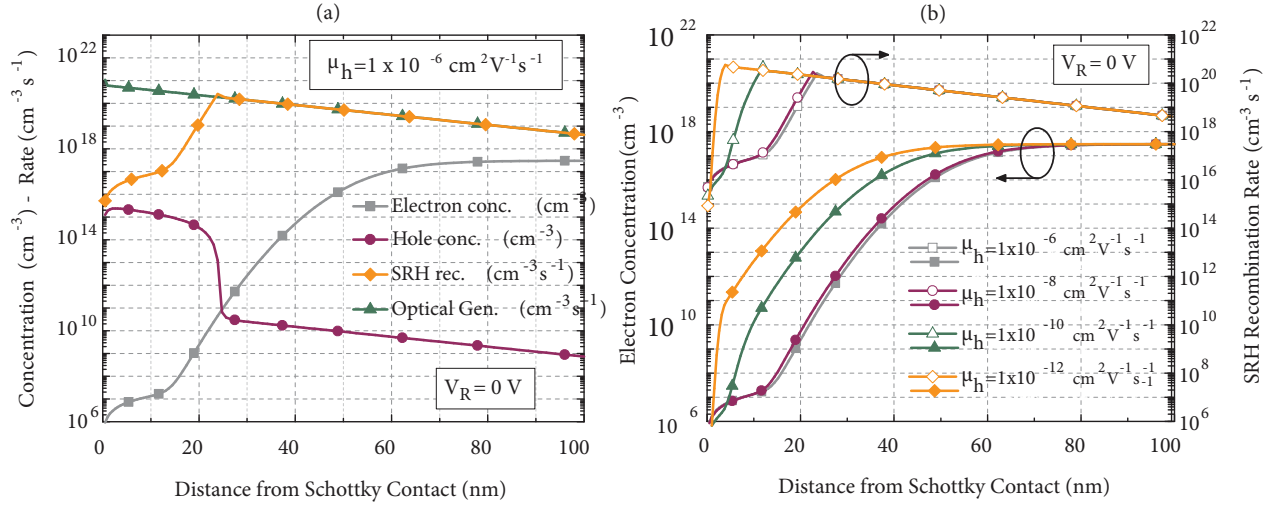


**Figure 2.** (a) Variation of electron and hole concentration and SRH and optical generation rate as a function of vertical distance from Schottky contact for hole mobility of  $1 \times 10^{-6} \text{ cm}^2\text{V}^{-1}\text{s}^{-1}$  under zero bias. (b) Electron concentration and SRH recombination rate for the diodes with hole mobility in the range of  $1 \times 10^{-6} \text{ cm}^2\text{V}^{-1}\text{s}^{-1} - 1 \times 10^{-12} \text{ cm}^2\text{V}^{-1}\text{s}^{-1}$  as a function of vertical distance from Schottky diode under zero bias.

To investigate the simulated electron concentration variation with hole mobility, it is wise to obtain hole profile across the device. Figure 3a shows variation of hole concentration as a function of distance from Schottky contact under different hole mobility. It can be seen that hole concentration at regions close to Schottky contact increases with decreasing hole mobility. Also, as expected from photo excitation profile, hole concentration shows exponential decay in the depletion region. Hole concentration values at the semiconductor-Schottky contact interface are obtained as follows;  $2 \times 10^{15} \text{ cm}^{-3}$ ,  $2 \times 10^{17} \text{ cm}^{-3}$ ,  $5 \times 10^{18} \text{ cm}^{-3}$  and  $6 \times 10^{19} \text{ cm}^{-3}$  at hole mobility values of  $1 \times 10^{-6} \text{ cm}^2\text{V}^{-1}\text{s}^{-1}$ ,  $1 \times 10^{-8} \text{ cm}^2\text{V}^{-1}\text{s}^{-1}$ ,  $1 \times 10^{-10} \text{ cm}^2\text{V}^{-1}\text{s}^{-1}$ ,

$1 \times 10^{-12} \text{ cm}^2\text{V}^{-1}\text{s}^{-1}$ , respectively. Due to charge neutrality condition, accumulation of holes require equal number of reduction in ionized donors which leads to depletion width narrowing. Note that  $N_D$  was set to  $3 \times 10^{17} \text{ cm}^{-3}$  thus, average hole concentration higher than  $N_D$  would significantly narrows the depletion width which is the case for very low hole mobility range ( $< 1 \times 10^{-8} \text{ cm}^2\text{V}^{-1}\text{s}^{-1}$ ). To conceive the accumulated hole level relation with hole mobility, current equations need to be visited. Electron ( $J_n$ ) and hole ( $J_p$ ) drift-diffusion current was calculated from the following equations;

$$J_n = qn\mu_n E + kT\mu_n \nabla n, \quad (4)$$

$$J_p = qp\mu_p E - kT\mu_p \nabla p, \quad (5)$$

where  $\mu_n$  and  $\mu_p$  are electron and hole mobility,  $E$  is electric field strength and  $\nabla n$  &  $\nabla p$  are concentration gradient of electrons & holes, respectively. One can see from Eq. (5) that drift component of hole current is directly proportional to 'p' and ' $\mu_p$ '. To satisfy similar drift current ' $\mu_p$ ' and 'p' need to be inversely proportional to each other which is exactly obtained for the hole mobility of  $1 \times 10^{-6} \text{ cm}^2\text{V}^{-1}\text{s}^{-1}$  and  $1 \times 10^{-8} \text{ cm}^2\text{V}^{-1}\text{s}^{-1}$ . However, further decrease in hole mobility resulted in relatively less increase in hole concentration. This phenomenon is related to the reduction in photo generated carriers within the depletion width. As discussed above, narrower depletion width was observed under very low hole mobility. Since hole current is dominated by drift component rather than diffusion (as seen in Figure 3b), reduction of depletion width directly scaled the total hole current. Inset to Figure 3b shows the variation of peak total hole current as a function of hole mobility. The reduction in hole current is in good agreement with the electron profiles (depletion width) shown in Figure 2b.

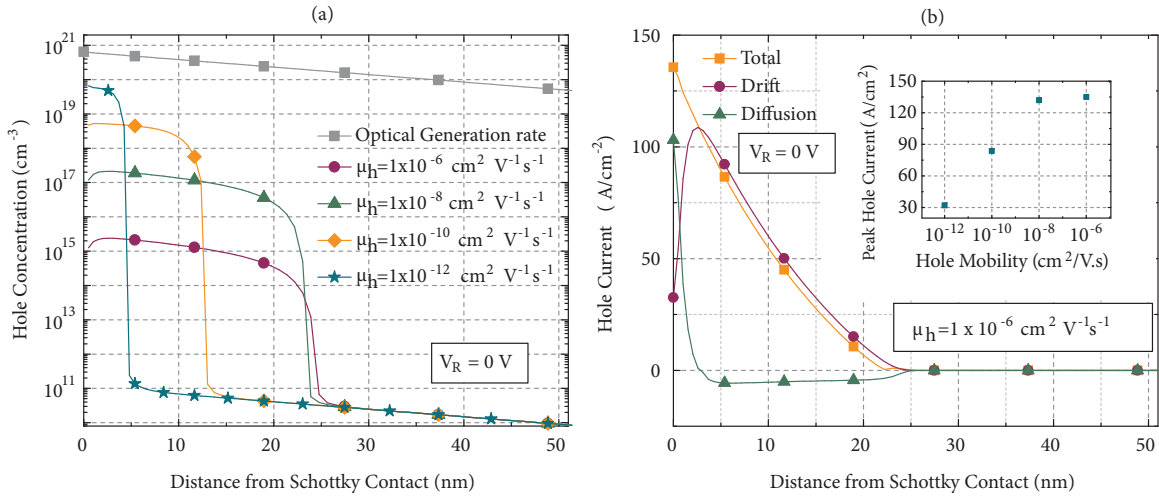


**Figure 3.** (a) Variation of hole concentration with respect to hole mobility in the range of  $1 \times 10^{-6} \text{ cm}^2\text{V}^{-1}\text{s}^{-1}$  -  $1 \times 10^{-12} \text{ cm}^2\text{V}^{-1}\text{s}^{-1}$  as a function of vertical distance from Schottky contact under zero bias. (b) Drift, diffusion and total hole current profile across the Schottky diode with hole mobility of  $1 \times 10^{-6} \text{ cm}^2\text{V}^{-1}\text{s}^{-1}$  under zero bias.

Having hole profile conceived for the investigated hole mobility range, electric field profile can be investigated as it is aimed to calculate SBL as a function of electric field (Eq. 1). Figure 4a shows the variation of electric field within the Schottky diode under varying hole mobility. In the case of hole mobility with

$1 \times 10^{-6} \text{ cm}^2\text{V}^{-1}\text{s}^{-1}$  and  $1 \times 10^{-8} \text{ cm}^2\text{V}^{-1}\text{s}^{-1}$ , electric field basically distributes almost same. Peak electric field near Schottky contact was obtained as 0.3 MV/cm. Such distribution is also similar to the one obtained under no UV excitation (not shown here). As expected this is due to low level hole accumulation in the depletion region compared to  $N_D$  value. On the other hand, sharp increase in electric field near Schottky contact is observed for extremely low hole mobility case ( $1 \times 10^{-10} \text{ cm}^2\text{V}^{-1}\text{s}^{-1}$  and  $1 \times 10^{-12} \text{ cm}^2\text{V}^{-1}\text{s}^{-1}$ ) which is in accordance with the high hole accumulation, well above  $N_D$  value (Figure 3a). Peak electric field near Schottky contact boosted to 0.91 MV/cm and 3 MV/cm for the cases with hole mobility of  $1 \times 10^{-10} \text{ cm}^2\text{V}^{-1}\text{s}^{-1}$  and  $1 \times 10^{-12} \text{ cm}^2\text{V}^{-1}\text{s}^{-1}$ , respectively (refer inset to Figure 4a). Note that all of these simulation results were obtained under zero bias condition. To have photoconductive gain, reverse bias should be applied in SBPs where excess electrons get thermionically injected into semiconductor upon barrier lowering due to high electric field in the semiconductor. Figure 4b shows variation of peak electric field at the Schottky-semiconductor interface as a function of reverse bias under varying hole mobility. In the case of hole mobility of  $1 \times 10^{-6} \text{ cm}^2\text{V}^{-1}\text{s}^{-1}$  and  $1 \times 10^{-8} \text{ cm}^2\text{V}^{-1}\text{s}^{-1}$ , as expected from a reverse biased Schottky junction, peak electric field strength approximately follows the relation (Figure 4b);

$$E = \sqrt{\frac{2qN_D(\Phi_i - V_R)}{\epsilon_s}}, \quad (6)$$

where  $\Phi_i$ ,  $V_R$  and  $\epsilon_s$  denotes built-in potential, reverse bias and dielectric constant of the junction. On the other hand, high positive charge accumulated under very low hole mobility ( $1 \times 10^{-10} \text{ cm}^2\text{V}^{-1}\text{s}^{-1}$  and  $1 \times 10^{-12} \text{ cm}^2\text{V}^{-1}\text{s}^{-1}$ ) leads to a dynamic charge profile where positive charge concentration changes as a function of reverse bias. This is in contrast to uniform charge profile in dark current conditions.

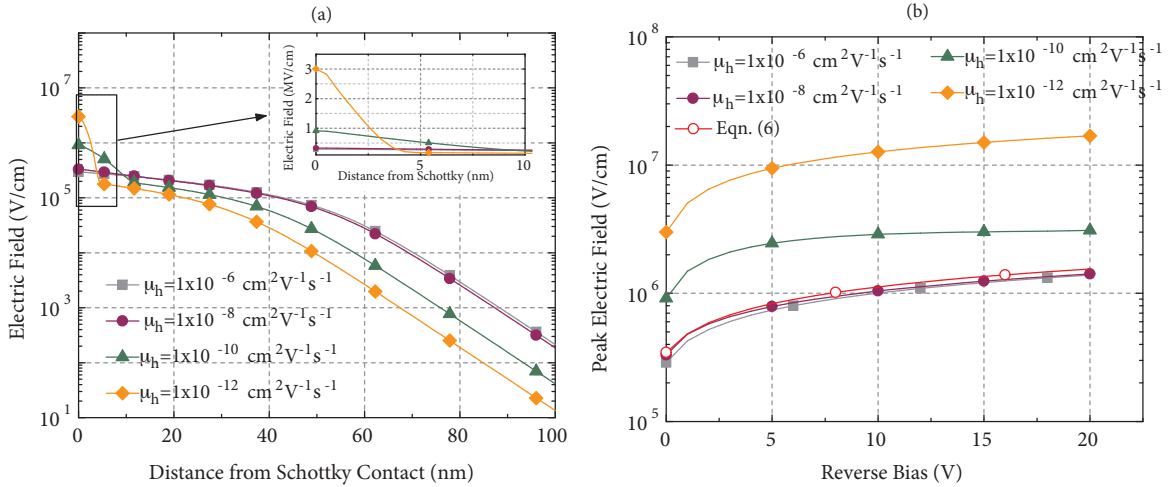


**Figure 4.** (a) Electric field profile across the Schottky diodes with hole mobility in the range of  $1 \times 10^{-6} \text{ cm}^2\text{V}^{-1}\text{s}^{-1}$  -  $1 \times 10^{-12} \text{ cm}^2\text{V}^{-1}\text{s}^{-1}$  under zero bias. (b) Variation of peak electric field as function of reverse bias for hole mobility in the range of  $1 \times 10^{-6} \text{ cm}^2\text{V}^{-1}\text{s}^{-1}$  -  $1 \times 10^{-12} \text{ cm}^2\text{V}^{-1}\text{s}^{-1}$ . The fit using Eq. 6 is also plotted.

As discussed in the methods section, following Eq. (1), SBL potential can be obtained using the peak electric field data shown in Figure 4b. Variation of the calculated SBL potential with reverse bias for different

hole mobility is plotted in Figure 5. It can be seen that for hole mobility higher than  $1 \times 10^{-8} \text{ cm}^2\text{V}^{-1}\text{s}^{-1}$ , Schottky barrier lowering can barely reached 0.14 eV at 20 V reverse bias. On the other hand, it increased to 0.20 eV and 0.43 eV at 10 V reverse bias for hole mobility of  $1 \times 10^{-10} \text{ cm}^2\text{V}^{-1}\text{s}^{-1}$  and  $1 \times 10^{-12} \text{ cm}^2\text{V}^{-1}\text{s}^{-1}$ , respectively. These values can be inserted into total photocurrent ( $I_{\text{ph}}^{\text{m}}$ ) equation that has two components; optically generated photo current ( $I_{\text{ph}}^{\text{o}}$ ) and thermionically injected electron current by using the following relation [33];

$$I_{\text{ph}}^{\text{m}} = \left[ e^{\frac{\Delta\phi_{\text{b}}}{kT}} - 1 \right] I_{\text{dark}} + I_{\text{ph}}^{\text{o}}. \quad (7)$$

Here, thermionically injected carriers are much higher for devices showing high internal gain compared to  $I_{\text{ph}}^{\text{o}}$ . Typical values reported in the literature for dark current and  $I_{\text{ph}}^{\text{m}}$  is on the order of 10  $\mu\text{A}$  (depends on applied reverse bias) and  $I_{\text{dark}}$  is  $\sim 10$  pA which requires  $\Delta\phi_{\text{b}}$  value around 0.3 eV to satisfy Eq. (7) [13, 34]. We can compare the calculated  $\Delta\phi_{\text{b}}$  values (Figure 5) with the estimated  $\Delta\phi_{\text{b}}$  value (0.3 eV) obtained through analytical fit to the experimental results of the  $\beta\text{-Ga}_2\text{O}_3$  based photodetectors. It can be seen that hole mobility less than  $1 \times 10^{-10} \text{ cm}^2\text{V}^{-1}\text{s}^{-1}$  is required in  $\beta\text{-Ga}_2\text{O}_3$  based photodetectors to accumulate enough number of holes near Schottky-semiconductor interface. Although  $1 \times 10^{-6} \text{ cm}^2\text{V}^{-1}\text{s}^{-1}$  of STH related hole mobility is theoretically calculated though DFT analysis, explaining experimentally observed photoconductive gain was found to require further lower hole mobility, less than  $1 \times 10^{-10} \text{ cm}^2\text{V}^{-1}\text{s}^{-1}$ . This indicates that other gain mechanisms can play role to explain gain mechanism unless such low hole mobility ( $1 \times 10^{-10} \text{ cm}^2\text{V}^{-1}\text{s}^{-1}$  -  $1 \times 10^{-12} \text{ cm}^2\text{V}^{-1}\text{s}^{-1}$ ) is reported by theoreticians or experimentalists. These processes include carrier multiplication under high electric field and SBL process through hole trapping near Schottky contact which are beyond the scope of this paper.

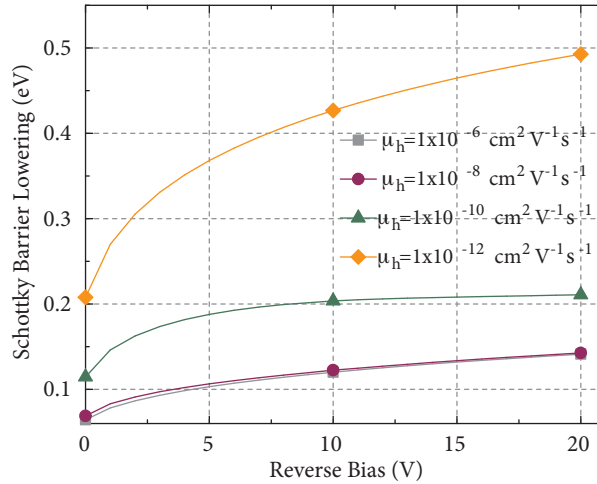


**Figure 5.** Calculated SBL potential for hole mobility in the range of  $1 \times 10^{-6} \text{ cm}^2\text{V}^{-1}\text{s}^{-1}$  -  $1 \times 10^{-12} \text{ cm}^2\text{V}^{-1}\text{s}^{-1}$  under varying reverse bias voltage.

To conclude, Silvaco Atlas software was used to model the effect of STH though low hole mobility ( $1 \times 10^{-6} \text{ cm}^2\text{V}^{-1}\text{s}^{-1}$  -  $1 \times 10^{-12} \text{ cm}^2\text{V}^{-1}\text{s}^{-1}$ ) in  $\beta\text{-Ga}_2\text{O}_3$  based vertical Schottky diodes. SRH recombination rate, hole concentration and current profiles were analysed and simulated results were discussed. Peak electric field values obtained under varying reverse bias with different hole mobility were used to calculate SBL

potential ( $\Delta\phi_b$ ). It was found that hole mobility less than  $1 \times 10^{-10} \text{ cm}^2\text{V}^{-1}\text{s}^{-1}$  is required to induce SBL of 0.3 eV which is the value obtained thorough analytical fit to the experimental results of  $\beta\text{-Ga}_2\text{O}_3$  based photodetectors. Unless such extremely low hole mobility is either experimentally or theoretically shown as STH mobility in  $\beta\text{-Ga}_2\text{O}_3$ , STH formation was found to be insufficient to explain overall photoconductive gain in  $\beta\text{-Ga}_2\text{O}_3$  based photodetectors.

### Acknowledgment

The author acknowledges the funding from The Scientific and Technological Council of Turkey (TÜBİTAK) (project number: 119F002).

### References

- [1] Tomm Y, Reiche P, Klimm D, Fukuda T. Czochralski grown Ga<sub>2</sub>O<sub>3</sub> crystals. *Journal of Crystal Growth* 2000; 220 (4): 510-514. doi:10.1016/S0022-0248(00)00851-4
- [2] Ohira S, Yoshioka M, Sugawara T, Nakajima K, Shishido T. Fabrication of hexagonal GaN on the surface of  $\beta\text{-Ga}_2\text{O}_3$  single crystal by nitridation with NH<sub>3</sub>. In: *Thin Solid Films*, Vol. 496. Amsterdam, Netherlands: Elsevier, 2006, pp. 53-57. doi: 10.1016/j.tsf.2005.08.230
- [3] Galazka Z, Irmscher K, Uecker R, Bertram R, Pietsch M et al. On the bulk  $\beta\text{-Ga}_2\text{O}_3$  single crystals grown by the Czochralski method. *Journal of Crystal Growth* 2014; 404: 184-191. doi: 10.1016/j.jcrysgro.2014.07.021
- [4] Villora EG, Shimamura K, Yoshikawa Y, Aoki K, Ichinose N. Large-size  $\beta\text{-Ga}_2\text{O}_3$  single crystals and wafers. *Journal of Crystal Growth* 2004; 270 (3-4): 420-426. doi: 10.1016/j.jcrysgro.2004.06.027
- [5] Kumar Saikumar A, Dhanraj S, Sundaram KB. Review-RF sputtered films of Ga<sub>2</sub>O<sub>3</sub>. *ECS Journal of Solid State Science and Technology* 2019; 8: 3064-3078. doi: 10.1149/2.0141907jss
- [6] Wei J, Kim K, Liu F, Wang P, Zheng X et al.  $\beta\text{-Ga}_2\text{O}_3$  thin film grown on sapphire substrate by plasma-assisted molecular beam epitaxy. *Journal of Semiconductors* 2019; 40. doi:10.1088/1674-4926/40/1/012802
- [7] Oshima Y, Villora EG, Shimamura K. Quasi-heteroepitaxial growth of  $\beta\text{-Ga}_2\text{O}_3$  on off-angled sapphire (0 0 1) substrates by halide vapor phase epitaxy. *Journal of Crystal Growth* 2015; 410: 53-58. doi: 10.1016/j.jcrysgro.2014.10.038
- [8] Zhang Y, Xia Z, Meqlone J, Sun W, Joichi J et al. Evaluation of low-temperature saturation modulation-doped field-effect transistors. *IEEE Transactions on Electron Devices* 2019; 66: 1574-1578. doi: 10.1109/TED.2018.2889573
- [9] Pratiyush AS, Krishnamoorthy S, Muralidharan R, Rajan S, Nath DN. Advances in Ga<sub>2</sub>O<sub>3</sub> solar-blind UV photodetectors. In: *Gallium Oxide: Technology, Devices and Applications*. Amsterdam, Netherlands: Elsevier, 2018, pp. 369-399. doi: 10.1016/B978-0-12-814521-0.00016-6
- [10] Qin Y, Li L, Zhao X, Tompa GS, Dong H et al. Metal-Semiconductor-Metal  $\epsilon\text{-Ga}_2\text{O}_3$  Solar-Blind Photodetectors with a Record-High Responsivity Rejection Ratio and Their Gain Mechanism. *ACS Photonics*. 2020;7:812-820. doi:10.1021/acsp Photonics.9b01727
- [11] Pratiyush AS, Krishnamoorthy S, Kumar S, Xia Z, Muralidharan R et al. MBE grown self-powered  $\beta\text{-Ga}_2\text{O}_3$  MSM deep-UV photodetector. *arXiv* 2018. arXiv:1802.01574.
- [12] Chen X, Xu Y, Zhou D, Yang S, Ren FF et al. Solar-blind photodetector with high avalanche gains and bias-tunable detecting functionality based on metastable phase  $\alpha\text{-Ga}_2\text{O}_3/\text{ZnO}$  isotype heterostructures. *ACS Applied Materials & Interfaces* 2017; 9: 36997-37005. doi: 10.1021/acsaami.7b09812
- [13] Oshima T, Okuno T, Arai N, Suzuki N, Ohira S et al. Vertical solar-blind deep-ultraviolet schottky photodetectors based on  $\beta\text{-Ga}_2\text{O}_3$  substrates. *Applied Physics Express* 2008; 1. doi: 10.1143/APEX.1.011202
- [14] Armstrong AM, Crawford MH, Jayawardena A, Ahyi A, Dhar S. Role of self-trapped holes in the photoconductive gain of  $\beta$ -gallium oxide Schottky diodes. *Journal of Applied Physics* 2016; 119: 1-7. doi: 10.1063/1.4943261

- [15] Varley JB, Janotti A, Franchini C, Van De Walle CG. Role of self-trapping in luminescence and p-type conductivity of wide-band-gap oxides. *Physical Review B* 2012; 85: 2-5. doi: 10.1103/PhysRevB.85.081109
- [16] Adnan MM, Verma D, Xia Z, Kalarickal NK, Rajan S et al. Spectral measurement of the breakdown limit of  $\beta$ -Ga<sub>2</sub>O<sub>3</sub> and field-dependent dissociation of self-trapped excitons and holes. *arXiv* 2020. arXiv:2011.00375.
- [17] Kananen BE, Giles NC, Halliburton LE, Foundos GK, Chang KB et al. Self-trapped holes in  $\beta$ -Ga<sub>2</sub>O<sub>3</sub> crystals. *Journal of Applied Physics* 2017; 122: 215703. doi: 10.1063/1.5007095
- [18] Frodason YK, Johansen KM, Vines L, Varley JB. Self-trapped hole and impurity-related broad luminescence in  $\beta$ -Ga<sub>2</sub>O<sub>3</sub>. *Journal of Applied Physics* 2020; 127: 075701. doi: 10.1063/1.5140742
- [19] Jiang ZX, Wu ZY, Ma CC, Deng JN, Zhang H et al. P-type  $\beta$ -Ga<sub>2</sub>O<sub>3</sub> metal-semiconductor-metal solar-blind photodetectors with extremely high responsivity and gain-bandwidth product. *Materials Today Physics* 2020; 14: 100226. doi: 10.1016/j.mtphys.2020.100226
- [20] Islam MM, Liedke MO, Winarski D, Butterling M, Wagner A et al. Chemical manipulation of hydrogen induced high p-type and n-type conductivity in Ga<sub>2</sub>O<sub>3</sub>. *Nature Scientific Reports* 2020; 10: 6134. doi: 10.1038/s41598-020-62948-2
- [21] Akyol F. Simulation of  $\beta$ -Ga<sub>2</sub>O<sub>3</sub> vertical Schottky diode based photodetectors revealing average hole mobility of  $20 \text{ cm}^2 \text{ V}^{-1} \text{ s}^{-1}$ . *Journal of Applied Physics* 2020; 127: 074501. doi: 10.1063/1.5136306
- [22] Takakura K, Koga D, Ohyama H, Rafi JM, Kayamoto Y et al. Evaluation of the crystalline quality of  $\beta$ -Ga<sub>2</sub>O<sub>3</sub> films by optical absorption measurements. *Physica B: Condensed Matter* 2009; 404 (23-24): 4854-4857. doi: 10.1016/j.physb.2009.08.167
- [23] Schottky W. Zur Halbleiterteorie der Sperrschicht- und Spitzengleichrichter. *Zeitschrift fur Physics* 1939; 113 (5-6): 367-414 (in German). doi: 10.1007/BF01340116
- [24] Mott NF. The theory of crystal rectifiers. *Proceedings of the Royal Society of London. Series A, Mathematical and Physical Sciences* 1939; 171: 27-38. doi: 10.1098/rspa.1939.0051
- [25] Lorenz MR, Woods JF, Gambino RJ. Some electrical properties of the semiconductor  $\beta$ -Ga<sub>2</sub>O<sub>3</sub>. *Journal of Physics and Chemistry of Solids* 1967; 28 (3): 403-404. doi: 10.1016/0022-3697(67)90305-8
- [26] Mohamed M, Irmscher K, Janowitz C, Galazka Z, Manzke R et al. Schottky barrier height of Au on the transparent semiconducting oxide  $\beta$ -Ga<sub>2</sub>O<sub>3</sub>. *Applied Physics Letters* 2012; 101: 132106. doi: 10.1063/1.4755770
- [27] Passlack M, Hunt NEJ, Schubert EF, Zydzik GJ, Mong M et al. Dielectric properties of electron-beam deposited Ga<sub>2</sub>O<sub>3</sub> films. *Applied Physics Letters* 1994; 64: 2715-2717. doi: 10.1063/1.111452
- [28] Oishi T, Koga Y, Harada K, Kasu M. High-mobility  $\beta$ -Ga<sub>2</sub>O<sub>3</sub> (-201) single crystals grown by edge-defined film-fed growth method and their Schottky barrier diodes with Ni contact. *Applied Physics Express* 2015; 8: 031101. doi: 10.7567/APEX.8.031101
- [29] Irmscher K, Galazka Z, Pietsch M, Uecker R, Fornari R. Electrical properties of  $\beta$ -Ga<sub>2</sub>O<sub>3</sub> single crystals grown by the Czochralski method. *Journal of Applied Physics* 2011; 110. doi: 10.1063/1.3642962
- [30] Korhonen E, Tuomisto F, Gogova D, Wagner G, Baldini M et al. Electrical compensation by Ga vacancies in Ga<sub>2</sub>O<sub>3</sub> thin films. *Applied Physics Letters* 2015; 106: 242103. doi: 10.1063/1.4922814
- [31] Alema F, Hertog B, Mukhopadhyay P, Zhang Y, Mauze A et al. Solar blind Schottky photodiode based on an MOCVD-grown homoepitaxial  $\beta$ -Ga<sub>2</sub>O<sub>3</sub> thin film. *Applied Physics Letters Materials* 2019; 7. doi: 10.1063/1.5064471
- [32] Shockley W, Read WT. Statistics of the recombinations of holes and electrons. *Physical Reviews* 1952; 87: 835-842. doi: 10.1103/PhysRev.87.835
- [33] Katz O, Garber V, Meyler B, Bahir G, Salzman J. Gain mechanism in GaN Schottky ultraviolet detectors. *Applied Physics Letters* 2001; 79: 1417-1419. doi: 10.1063/1.1394717
- [34] Singh Pratiyush A, Krishnamoorthy S, Vishnu Solanke S, Zhanbo X, Muralidharan R et al. High responsivity in molecular beam epitaxy grown  $\beta$ -Ga<sub>2</sub>O<sub>3</sub> metal semiconductor metal solar blind deep-UV photodetector. *Applied Physics Letters* 2017; 110: 1-6. doi: 10.1063/1.4984904